J|A|C|S
ARTICLES
Published on Web 08/17/2002

The Active Site of a Zinc-Dependent Metalloproteinase Influences the Computed pK_a of Ligands Coordinated to the Catalytic Zinc Ion

Jason B. Cross,† José S. Duca,* James J. Kaminski, and Vincent S. Madison

Contribution from the Department of Structural Chemistry, Schering-Plough Research Institute, 2015 Galloping Hill Road, Kenilworth, New Jersey 07033

Received February 4, 2002

Abstract: TNF-α converting enzyme (TACE) is a multidomain, membrane-anchored protein that includes a Zn-dependent protease domain. It releases the soluble form of cytokine tumor necrosis factor-α (TNF-α) from its membrane-bound precursor. TACE is a metalloprotease containing a catalytic glutamic acid, Glu-406, and a Zn^{2+} ion ligated to three imidazoles. The protonation states of the active site glutamic acid and inhibitors are important factors in understanding the potency of inhibitors with acidic zinc-ligating groups such as hydroxamic and carboxylic acids. Density functional methods were utilized to compute pK_a values using a model of the catalytic site of TACE and to predict a concomitant mechanism of binding, consistent with lowering the pK_a of the bound ligand and raising the pK_a of the active site Glu-406. Weak acids, such as hydroxamic acids, bind in their neutral form and then transfer an acidic proton to Glu-406. Stronger acids, such as carboxylic acids, bind in their anionic form and require preprotonation of Glu-406. Similar binding events would be expected for other zinc-dependent proteases.

Introduction

Tumor necrosis factor-α (TNF-α) is an important cytokine, responsible for initiating protective inflammatory reactions. However, it also plays a role in the development of many diseases. Rheumatoid arthritis, diabetes, endotoxic shock, and HIV cachexia can all result from the excess production of TNF-α.[1] Increased TNF-α production has also been linked to advanced cardiac dysfunction in myocarditis,[2,3] osteoarthritis,[4] and neural damage from the inflammatory response due to bacterial meningitis infection.[5,6] Given these complications, the reduction of TNF-α activity is an appealing therapeutic goal.

Tumor necrosis factor-α converting enzyme (TACE) is a zinc endopeptidase that releases soluble TNF-α from its membrane-bound precursor[7−10] through proteolysis of the Ala-76 → Val-77 bond[11] by membrane-bound TACE.[12,13] Since it is the soluble form of TNF-α that is responsible for its cytokine activity, inhibition of TACE is an attractive scheme for reducing the production of active TNF-α. In fact, there has recently been a great deal of interest in the development of inhibitors for TACE.[14−18]

* To whom correspondence should be addressed. E-mail: jose.duca@spcorp.com.

† Current address: Department of Chemistry, Wayne State University, Detroit, MI 48202.

(1) Moss, M. L.; White, J. M.; Lambert, M. H.; Andrews, R. C. *Drug Discovery Today* **2001**, *6*, 417−426.
(2) Satoh, M.; Nakamura, M.; Satoh, H.; Segawa, I.; Masuda, T.; Hiramori, K. *Circulation* **1999**, *100*, 381−381.
(3) Satoh, M.; Nakamura, M.; Satoh, H.; Saitoh, H.; Segawa, I.; Hiramori, K. *J. Am. Coll. Cardiol.* **2000**, *36*, 1288−1294.
(4) Amin, A. R. *Osteoarthritis Cartilage* **1999**, *7*, 392−394.
(5) Leib, S. L.; Clements, J. M.; Lindberg, R. L. P.; Heimgartner, C.; Loeffler, J. M.; Pfister, L. A.; Tauber, M. G.; Leppert, D. *Brain* **2001**, *124*, 1734−1742.
(6) Leib, S. L.; Leppert, D.; Clements, J.; Tauber, M. G. *Infect. Immunol.* **2000**, *68*, 615−620.
(7) Mohler, K. M.; Sleath, P. R.; Fitzner, J. N.; Cerretti, D. P.; Alderson, M.; Kerwar, S. S.; Torrance, D. S.; Ottenevans, C.; Greenstreet, T.; Weerawarna, K.; Kronheim, S. R.; Petersen, M.; Gerhart, M.; Kozlosky, C. J.; March, C. J.; Black, R. A. *Nature* **1994**, *370*, 218−220.
(8) Black, R. A.; Durie, F. H.; OttenEvans, C.; Miller, R.; Slack, J. L.; Lynch, D. H.; Castner, B.; Mohler, K. M.; Gerhart, M.; Johnson, R. S.; Itoh, Y.; Okada, Y.; Nagase, H. *Biochem. Biophys. Res. Commun.* **1996**, *225*, 400−405.
(9) Black, R. A.; Rauch, C. T.; Kozlosky, C. J.; Peschon, J. J.; Slack, J. L.; Wolfson, M. F.; Castner, B. J.; Stocking, K. L.; Reddy, P.; Srinivasan, S.; Nelson, N.; Boiani, N.; Schooley, K. A.; Gerhart, M.; Davis, R.; Fitzner, J. N.; Johnson, R. S.; Paxton, R. J.; March, C. J.; Cerretti, D. P. *Nature* **1997**, *385*, 729−733.
(10) Moss, M. L.; Jin, S. L. C.; Milla, M. E.; Burkhart, W.; Carter, H. L.; Chen, W. J.; Clay, W. C.; Didsbury, J. R.; Hassler, D.; Hoffman, C. R.; Kost, T. A.; Lambert, M. H.; Leesnitzer, M. A.; McCauley, P.; McGeehan, G.; Mitchell, J.; Moyer, M.; Pahel, G.; Rocque, W.; Overton, L. K.; Schoenen, F.; Seaton, T.; Su, J. L.; Warner, J.; Willard, D.; Becherer, J. D. *Nature* **1997**, *385*, 733−736.
(11) Maskos, K.; Fernandez-Catalan, C.; Huber, R.; Bourenkov, G. P.; Bartunik, H.; Ellestad, G. A.; Reddy, P.; Wolfson, M. F.; Rauch, C. T.; Castner, B. J.; Davis, R.; Clarke, H. R. G.; Petersen, M.; Fitzner, J. N.; Cerretti, D. P.; March, C. J.; Paxton, R. J.; Black, R. A.; Bode, W. *Proc. Natl. Acad. Sci. U.S.A.* **1998**, *95*, 3408−3412.
(12) Reddy, P.; Slack, J. L.; Davis, R.; Cerretti, D. P.; Kozlosky, C. J.; Blanton, R. A.; Shows, D.; Peschon, J. J.; Black, R. A. *J. Biol. Chem.* **2000**, *275*, 14608−14614.
(13) Itai, T.; Tanaka, M.; Nagata, S. *Eur. J. Biochem.* **2001**, *268*, 2074−2082.
(14) Rabinowitz, M. H.; Andrews, R. C.; Becherer, J. D.; Bickett, D. M.; Bubacz, D. G.; Conway, J. G.; Cowan, D. J.; Gaul, M.; Glennon, K.; Lambert, M. H.; Leesnitzer, M. A.; McDougald, D. L.; Moss, M. L.; Musso, D. L.; Rizzolio, M. C. *J. Med. Chem.* **2001**, *44*, 4252−4267.
(15) Xue, C. B.; He, X. H.; Corbett, R. L.; Roderick, J.; Wasserman, Z. R.; Liu, R. Q.; Jaffee, B. D.; Covington, M. B.; Qian, M. X.; Trzaskos, J. M.; Newton, R. C.; Magolda, R. L.; Wexler, R. R.; Decicco, C. P. *J. Med. Chem.* **2001**, *44*, 3351−3354.
(16) Levin, J. I.; Chen, J.; Du, M.; Hogan, M.; Kincaid, S.; Nelson, F. C.; Venkatesan, A. M.; Wehr, T.; Zask, A.; DiJoseph, J.; Killar, L. M.; Skala, S.; Sung, A.; Sharr, M.; Roth, C.; Jin, G.; Cowling, R.; Mohler, K. M.; Black, R. A.; March, C. J.; Skotnicki, J. S. *Bioorg. Med. Chem. Lett.* **2001**, *11*, 2189−2192.
(17) Barlaam, B.; Bird, T. G.; Lambert-van der Brempt, C.; Campbell, D.; Foster, S. J.; Maciewicz, R. *J. Med. Chem.* **1999**, *42*, 4890−4908.

10.1021/ja0201810 CCC: $22.00

Ligand geometry and protonation states are important factors for inhibitor design. Binding geometries of non-hydrogen atoms are well defined by X-ray crystallography of enzyme/inhibitor complexes. In this study, theoretical methods were used to reproduce the known binding geometry of a ligand, to predict the bound geometry of a second ligand, and to predict protonation states and pK_a values for ligands and TACE groups. The 2.0-Å X-ray crystal structure of TACE cocrystallized with a hydroxamic acid inhibitor, 3,*N*-{(*R*,*S*)-[2-(hydroxyaminocarbonyl)methyl]-4-methylpentanoyl}-(*S*)-3-(*tert*-butyl)glycyl-(*S*)-alanoyldiethylene amide (**1**)[11] served as a structural template

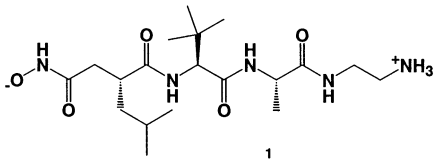

1

for calculations of stationary point geometries. Since predictions of protonation states are inaccessible by most experimental methods, we have used density functional methods to compute pK_a values for several ligand and TACE active site functional groups. These calculations provide the basis for understanding the changes that occur in the active site environment during the approach and coordination of potential inhibitors.

Computational Methods

Calculations were performed using the Jaguar 4.1 program.[19] Geometry optimizations were carried out using the B3LYP hybrid density functional[20−22] with the LACVP* pseudopotential[23] used on the zinc ion and the 6-31G* basis set used on all other atoms.

pK_a calculations were performed using the pK_a prediction module[24,25] in Jaguar 4.1, which is based on a closed thermodynamic cycle.

$$\begin{array}{ccccc} AH_{(g)} & \xrightarrow{\Delta G_1} & A^-_{(g)} & + & H^+_{(g)} \\ \downarrow \Delta G_3 & & \downarrow \Delta G_4 & & \downarrow \Delta G_{H^+(sol)} \\ AH_{(aq)} & \xrightarrow[\Delta G_2]{} & A^-_{(aq)} & + & H^+_{(aq)} \end{array}$$

This module computes a raw pK_a value for a protonated structure, AH, using eqs 1−4,[25] with an added empirical correction shown in eq 5.

$$pK_{a(raw)} = \Delta G_2/2.3RT = (\Delta G_1 + \Delta G_4 + \Delta G_{H^+(sol)} - \Delta G_3)/2.3RT \quad (1)$$

$$\Delta G_1 = \Delta H_{(gas)} - T\Delta S_{(gas)} = E_{A^-(gas)} - E_{AH\,(gas)} + 5/2RT - T\Delta S_{(gas)} \quad (2)$$

$$\Delta G_3 = \Delta G_{AH\,(sol)} \quad (3)$$

$$\Delta G_4 = \Delta G_{A^-(sol)} \quad (4)$$

$$pK_a = CpK_{a(raw)} + D \quad (5)$$

$E_{X(gas)}$ is computed with the B3LYP/cc-pVTZ(-f)[+]//B3LYP/6-31G-[**] method,[26−28] and $\Delta G_{X(sol)}$ is computed with the self-consistent reaction field continuum solvation method[29] using B3LYP/6−31[+]-G**//B3LYP/6-31G[**]. The functions in brackets are applied to the atoms involved in deprotonation. The LACVP basis set, with appropriate polarization functions, is included for the zinc atom. The experimental value for $\Delta G_{H^+(sol)}$ of −259.5 kcal/mol is used.[30] $T\Delta S_{(gas)}$ is approximated by the value 7.8 kcal/mol, based on the reported entropy of a proton.[31]

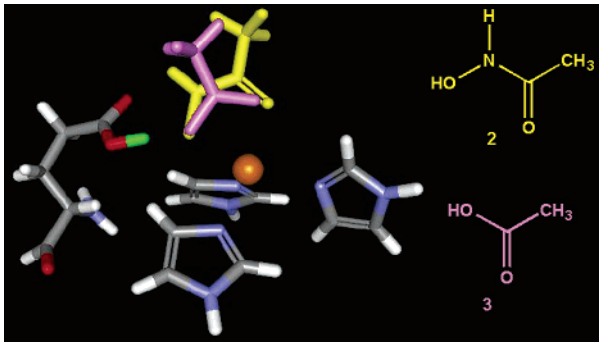

Figure 1. TACE active site computational model based on the X-ray crystal structure. Acetate anion (magenta) and acetohydroxamate anion (yellow) were geometry optimized while the active site structure was held fixed. The pK_a for the Glu-406 acid proton (green) was calculated for a series of active site models.

As models of the TACE active site, molecular fragments from the TACE complex with **1** were extracted from the PDB file 1BKC. All models included three imidazole rings representing His-405, His-409, and His-415 and the catalytic zinc ion (Zn^{2+}), abbreviated $Zn(Imd)_3$. For geometry optimization, the anion of Glu-406 was represented by the formate anion. The pK_a calculations were done for isolated acids, for a partial active site model [$Zn(Imd)_3$], or for a "complete" active site model comprising $Zn(Imd)_3$ plus the complete Glu-406 residue with capped end groups. For all of the calculations, the coordinates of the active site models were fixed.

Results and Discussion

Acetohydroxamic acid (**2**) (a model for the hydroxamic acid inhibitor) and acetic acid (**3**) were geometry optimized in the active site model allowing both ligand mobility and proton transfer. The calculated binding modes for acetohydroxamic acid and acetic acid are illustrated in Figure 1.

The RMSD for the heavy atoms of acetohydroxamic acid compared to the corresponding atoms of the inhibitor is 0.17 Å, which suggests the active site model can reproduce the inhibitor interactions within the binding pocket of TACE. Acetohydroxamic acid displays bidentate coordination to zinc. There is proton transfer from acetohydroxamic acid to the formate (Glu-406) anion with subsequent hydrogen bonding between the Glu-406 acid proton and the hydroxyl oxygen of the hydroxamate anion. Another hydrogen-bonding interaction is predicted between the NH proton of the hydroxamate anion

(18) Whittaker, M.; Floyd, C. D.; Brown, P.; Gearing, A. J. H. *Chem. Rev.* **1999**, *99*, 2735−2776.
(19) Schrodinger, Inc.: Portland, OR, 1991−2000.
(20) Becke, A. D. *Phys. Rev. A* **1988**, *38*, 3098−3100.
(21) Becke, A. D. *J. Chem. Phys.* **1993**, *98*, 5648−5652.
(22) Lee, C. T.; Yang, W. T.; Parr, R. G. *Phys. Rev. B* **1988**, *37*, 785−789.
(23) Hay, P. J.; Wadt, W. R. *J. Chem. Phys.* **1985**, *82*, 299−310.
(24) Klicic, J. J.; Perry, J. K.; Ringnalda, M. N. *Abstr. Pap. Am. Chem. Soc.* **1998**, *215*, U540−U540.
(25) Klicic, J. J.; Friesner, R. A.; Liu, S. Y.; Guida, W. C. *J. Phys. Chem. A* **2002**, *106*, 1327−1335.
(26) Kendall, R. A.; Dunning, T. H.; Harrison, R. J. *J. Chem. Phys.* **1992**, *96*, 6796−6806.
(27) Dunning, T. H. *J. Chem. Phys.* **1989**, *90*, 1007−1023.
(28) Woon, D. E.; Dunning, T. H. *J. Chem. Phys.* **1993**, *98*, 1358−1371.
(29) Marten, B.; Kim, K.; Cortis, C.; Friesner, R. A.; Murphy, R. B.; Ringnalda, M. N.; Sitkoff, D.; Honig, B. *J. Phys. Chem.* **1996**, *100*, 11775−11788.
(30) Reiss, H.; Heller, A. *J. Phys. Chem.* **1985**, *89*, 4207−4213.
(31) Lim, C.; Bashford, D.; Karplus, M. *J. Phys. Chem.* **1991**, *95*, 5610−5620.

Scheme 1. Proposed Binding Mechanism of Acetohydroxamic Acid in the TACE Active Site (w = H_2O)

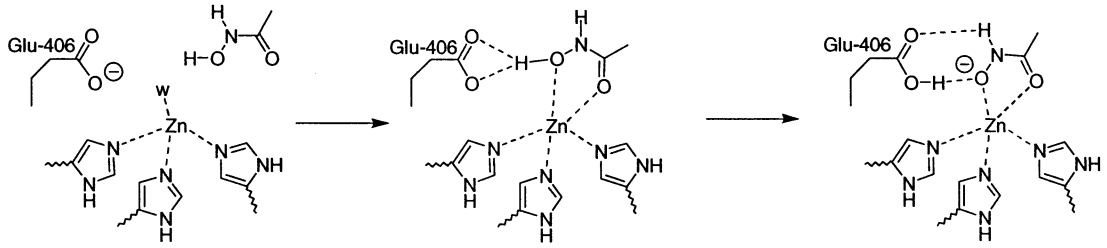

Scheme 2. Proposed Binding Mechanism of Acetic Acid in the TACE Active Site (w = H_2O)

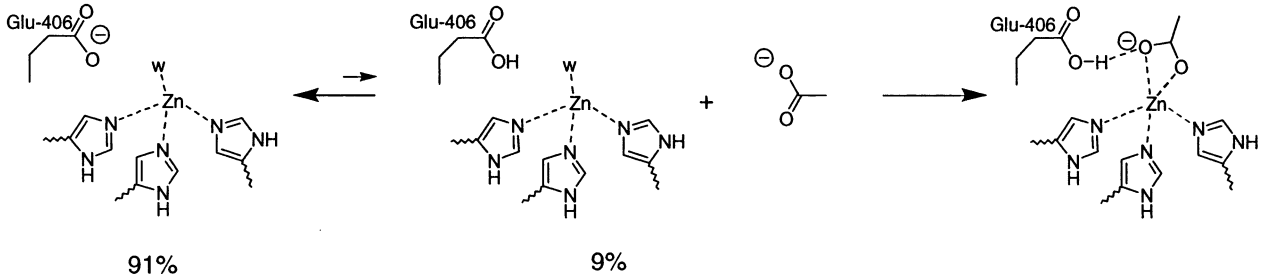

Table 1. Calculated and Experimental pK_a Values for Glutamic Acid, Acetohydroxamic Acid, and Acetic Acid Protons in the Absence and Presence of the TACE Active Site

structure	calcd pK_a	exptl pK_a
Glu-406	4.1	4.3
Glu-406 + $Zn(Imd)_3$ + H_2O	6.5	
Glu-406 + $Zn(Imd)_3$ + acetohydroxamate	5.9	
Glu-406 + $Zn(Imd)_3$ + acetate	6.2	
acetohydroxamic acid	8.4	8.7
acetohydroxamic acid + $Zn(Imd)_3$	5.1	
acetic acid	3.7	4.7
acetic acid + $Zn(Imd)_3$	1.4	

and the unprotonated carboxylate oxygen of Glu-406. In the crystal structure, the hydroxamate nitrogen is equidistant between the carboxylate oxygen and the backbone carbonyl oxygen of Gly-131.

The optimized geometry of acetate places the two oxygens close to those of the hydroxamate, giving bidentate ligation with equivalent Zn−O distances. Once more, the acidic proton is transferred from the model inhibitor to the formate anion (Glu-406). There are no published X-ray structures for carboxylic acids binding to TACE. Analysis of zinc binding sites in protein crystal structures has shown that both monodentate and bidentate ligation are common for carboxylic acids.[32] Recently, the ab initio methods employed herein successfully reproduced the geometry of carboxylate inhibitors complexed with another metalloprotease (peptide deformylase).[33]

The pK_a values, Table 1, for acidic protons in proteins are difficult to measure experimentally. The accurate reproduction of the experimental binding geometry of a hydroxamate inhibitor was a prerequisite for the computation of pK_a values for various acidic protons in our models.

The pK_a value computed for the acidic proton of isolated glutamic acid is 4.1, which is comparable to its experimentally determined value of 4.3.[34] From a study of MMP-3 catalysis and inhibition,[35] a pK_a of 5.6 has been assigned to the catalytic glutamic acid residue, which is in agreement with previous experimental work on carboxypeptidase A.[36,37] This shift to a more neutral value compared to the isolated residue is mimicked by the calculated pK_a of 6.5 for the complete active site model with a water molecule as the zinc ligand.

Acetohydroxamic acid was used to calculate a representative pK_a value for this group of inhibitors. The use of this model compound lowered the computational cost while preserving the binding mode geometry of the hydroxamic acid functional group, Figure 1. The computed pK_a value of isolated acetohydroxamic acid is 8.4, which is in agreement with its experimentally determined value of 8.7.[34] The computed pK_a value of acetohydroxamic acid using the partial active site model was 5.1, which is significantly more acidic than the uncoordinated acetohydroxamic acid. Using the complete active site model and hydroxamate anion, the pK_a value for Glu-406 was calculated as 5.9. These pK_a values are consistent with transfer of the acidic proton from hydroxamic acid to the carboxylate group of Glu-406 as also predicted by the geometry optimization. Based on these calculations, a generalized binding mechanism for a hydroxamic acid inhibitor in the TACE active site is proposed, Scheme 1, in which the inhibitor replaces a water molecule in the zinc coordination sphere.[11]

Following the protocol outlined for acetohydroxamic acid, additional calculations were performed using acetic acid as the coordinating ligand. The calculated pK_a value of isolated acetic acid, 3.7, also agrees fairly well with its experimentally determined value of 4.7.[34] When computed using the partial active site model, the pK_a value of acetic acid is reduced to 1.4. The pK_a of Glu-406 in the presence of acetate is 6.2 when the complete active site model is used. The relative pK_a values indicate that Glu-406 should be protonated prior to binding carboxylate inhibitors, as indicated in Scheme 2. Thus, the carboxylate anion can bind only to the lower population of TACE with protonated Glu-406 at neutral pH (approximately

(32) Alberts, I. L.; Nadassy, K.; Wodak, S. J. *Protein Sci.* **1998**, *7*, 1700−1716.
(33) Madison, V.; Duca, J.; Bennett, F.; Bohanon, S.; Cooper, A.; Chu, M.; Desai, J.; Girijavallabhan, V.; Hare, R.; Hruza, A.; Hendrata, S.; Huang, Y.; Kravec, C.; Malcolm, B.; McCormick, J.; Miesel, L.; Ramanathan, L.; Reichert, P.; Saksena, A.; Wang, J.; Weber, P. C.; Zhu, H.; Fischmann, T. *Biophys. Chem.*, in press.
(34) *The Merck Index*; 12 ed.; Merck Research Laboratories: Rahway, NJ, 1996.
(35) Johnson, L. L.; Pavlovsky, A. G.; Johnson, A. R.; Janowicz, J. A.; Man, C. F.; Ortwine, D. F.; Purchase, C. F.; White, A. D.; Hupe, D. J. *J. Biol. Chem.* **2000**, *275*, 11026−11033.
(36) Hass, G. M.; Neurath, H. *Biochemistry* **1971**, *10*, 3535.
(37) Hass, G. M.; Neurath, H. *Biochemistry* **1971**, *10*, 3541.

9% taking the experimental pK_a of 5.6 for the active site glutamic acid of MMP-3[35]). This requirement for protonation is thought to be partially responsible for the generally lower affinity that carboxylic acids show toward MMPs in comparison to hydroxamic acids.[33]

Conclusions

Our calculations suggest that binding to the zinc ion (Zn^{2+}) within the binding cavity of TACE lowers the pK_a of hydroxamic and carboxylic acids. This proposal is consistent with experimental evidence that zinc-bound water molecules in MMPs present a decreased pK_a.[38] In addition, the calculations suggest that the binding events can be delineated into two complementary steps: (1) binding to the coordinated zinc ion decreases the pK_a of the ligand (3.3 and 2.3 units for hydroxamic and acetic acid, respectively) and (2) hydrogen-bonding and electrostatic interactions raise the pK_a of Glu-406 (1.8 and 2.1 units, respectively).

A detailed understanding of the binding process occurring within binding sites can be utilized to design more efficient inhibitors. In that sense, the ability to compute *microscopic* pK_a values within a binding cavity environment can contribute significantly to the design of more potent novel therapeutic agents. While the findings reported herein have concentrated on the binding events occurring in TACE, similar processes would be expected for other zinc-dependent proteases.

Acknowledgment. We thank Professor H. Bernhard Schlegel, Dr. Patricia Weber, and the Schering Plough Research Institute for their support of J.B.C. as a Summer Research Intern.

Supporting Information Available: Cartesian coordinates of protonated and unprotonated structures used to compute pK_a's. This material is available free of charge via the Internet at http://pubs.acs.org. See any current masthead page for ordering information and Web access instructions.

JA0201810

(38) Lipscomb, W. N.; Strater, N. *Chem. Rev.* **1996**, *96*, 2375−2433.